Received May 23, 2020, accepted June 14, 2020, date of publication July 9, 2020, date of current version July 27, 2020.

Digital Object Identifier 10.1109/ACCESS.2020.3008322

Transient Thermal Responses of Skin to Pulsed Millimeter Waves

KENNETH R. FOSTER[1], (Life Fellow, IEEE), MARVIN C. ZISKIN[2], (Life Fellow, IEEE), QUIRINO BALZANO[3], (Life Fellow, IEEE), AND AKIMASA HIRATA[4], (Fellow, IEEE)

[1]Department of Bioengineering, University of Pennsylvania, Philadelphia, PA 19104, USA
[2]Department of Radiology, Temple University Medical School, Philadelphia, PA 19140, USA
[3]Department of Electrical and Computer Engineering, University of Maryland, College Park, MD 20742, USA
[4]Department of Electrical and Mechanical Engineering, Nagoya Institute of Technology, Nagoya 466-8555, Japan

Corresponding author Kenneth R. Foster (kfoster@seas.upenn.edu)

The work of Kenneth R. Foster, Marvin C. Ziskin, and Quirino Balzano was supported in part by the Mobile & Wireless Forum.

ABSTRACT This study examines thermal responses of skin to pulsed millimeter wave (mm-wave) and radiofrequency (RF) radiation. We review limits for pulse fluence in the IEEE Std. C95.1-2019 and the 2020 guideline of the International Commission on Nonionizing Radiation Protection (ICNIRP), as well as the recently re-affirmed guidelines of the U.S. Federal Communications Commission (FCC). The focus of the study is on millimeter-wave frequencies (30-300 GHz) where energy is absorbed close to the body surface and intense pulses could potentially cause high temperature gradients at the skin, but the model is extended to lower frequencies as well. The study employs a simple one-dimensional baseline thermal model for skin and Pennes' bioheat equation (BHTE), together with a baseline model for thermal damage to skin based on a standard model. The predicted temperature increases produced by 3-sec pulses at 94 GHz are consistent with previous experimental results with no adjustable parameters in the model. The few reported data on thermal damage to the skin from pulsed 94 GHz energy are insufficient to enable a conventional analysis of damage thresholds and the data may be affected by errors in dosimetry. The baseline model suggests that the implicit limits on pulse fluence in the present FCC guidelines might allow, in extreme (but in practice unrealistic) cases, transient increases in skin temperature that approach thresholds for thermal pain but which remain well below levels anticipated to cause thermal damage. Limits on pulse fluence in the current IEEE and ICNIRP exposure guidelines would preclude such effects. Such extreme pulses are far above those that are emitted by wireless and other technologies but may be emitted by some nonlethal weapons systems. FCC's proposed ''device-based time averaging'' rules will restrict thermal transients in skin from mm-wave transmitters to levels that are roughly an order of magnitude below the slower temperature increases produced by the low-frequency components of the modulation waveform and appear to be excessively conservative. An appendix discusses the applicability of two approximations to the analytical solutions to the bioheat equation that can be used to estimate temperature increases in skin from exposure to mm-waves.

INDEX TERMS Radiofrequency safety, millimeter waves, exposure limits, bioheat equation, thermal damage, hazard.

I. INTRODUCTION

Two major international exposure guidelines for radiofrequency (RF) energy (International Commission on Nonionizing Radiation Protection, ICNIRP (2020) [1] and IEEE C95.1-2019 [2]) have been recently updated, while the U.S. Federal Communications Commission (FCC) has recently announced that its present RF exposure limits [3] will be continued without revision. The IEEE and ICNIRP limits were explicitly designed to protect against identified hazards of RF energy, which at frequencies above about 100 kHz are thermal in nature. The FCC limits evolved from a combination of an earlier (1991) edition of the IEEE limits and the recommendations in a 1986 report of the National Council on Radiation Protection and Measurements (NCRP) [4] and similarly have a thermal basis. These three limits are summa-

The associate editor coordinating the review of this manuscript and approving it for publication was Pu-Kun Liu.

rized in Table 1 at frequencies above about 1 GHz through the millimeter wave (mm-wave) range of 30-300 GHz.

All three exposure guidelines establish ''averaging times'' for exposure to account for the thermal response time of the body. In IEEE C95.1-2019 and ICNIRP (2020) these averaging times are 30 min for whole body exposure, and 6 min for ''local exposures'' from sources located close to the body. These reflect differences in thermal inertia of the whole body vs. limbs. The FCC provides averaging times for the MPE (maximum permissible exposure) of 6 and 30 min for occupational and general public exposures, respectively but the thermal rationale for these differences is not explicitly stated.

Millimeter waves have a very short energy penetration depth into the skin, <0.5 mm, with correspondingly high exposure to skin (high Specific Absorption Rates or SARs) for a given incident power density. However, skin is a very leaky reservoir for heat, with high rates of thermal conduction into deeper layers of tissue and, to a lesser extent, loss of heat back to the environment due to convective and evaporative cooling. Heat conducted into subcutaneous tissue is removed by blood perfusion to the body core. If energy is pushed quickly into skin (e.g. from a high-fluence mm-wave pulse), its temperature rise is limited by conduction into deeper layers of tissue, whereas at lower rates of heating (from more moderate exposures), the increase in skin temperature is chiefly limited by the rate of removal of heat from subcutaneous tissues to the body core. These two processes occur on significantly different time scales, ranging from seconds to several minutes.

To avoid excessive heating of skin by mm-waves, both IEEE C95.1-2019 and ICNIRP (2020) limit the fluence (incident power density times pulse width) of RF pulses, in addition to local and whole-body exposure limits. While FCC has no explicit limits on fluence of RF pulses, its exposure guidelines implicitly limit pulse fluence to the product of MPE (maximum permissible exposure) and averaging time, which amounts to 18 kJ/m^2 for both occupational and general public exposures. Some authors have argued that these limits are insufficient to prevent excessive heating from RF pulses from wireless devices operating above 10 GHz [5], [6]. Many websites have echoed these concerns and assert that ''short temperature spikes in the skin'' can be produced by 5G communications technology, some of which transmits in the mm-wave band as well as at lower RF frequencies.

This paper extends our recent analysis [7]–[9] of the thermal response of skin to RF energy using a simple model based on solutions of Pennes' bioheat equation (BHTE) focusing on frequencies above 6 GHz, where energy is deposited close to the body surface. Some of the analytical results presented below were previously reported but are repeated for clarity of presentation. We present the model as a baseline for more precise models and use standard parameter values, without adjusting the model parameters or doing post-hoc data fitting (which would introduce overfitting into the model).

We consider the thermal transients produced in skin by mm-wave pulses of the maximum fluence compliant with FCC exposure limits. These represent hypothetical worst cases that are far beyond anything that is possible from ordinary civilian technologies, but may be produced by non-lethal weapons systems (Active Denial [10], [11] or a lower powered civilian version called Silent Guardian [12]) that beam high-fluence mm-wave pulses at the target with the purpose of eliciting thermal pain without burning the skin. A related issue, temperature elevations from extreme localized exposures that may be compliant with spatial averaging provisions in the limits, is not considered here. To avoid misunderstanding, only thermal hazards are considered; the controversial issue of ''nonthermal'' effects would require a separate analysis.

II. THERMAL MODEL

The thermal response of skin is calculated from Pennes' bioheat equation (BHTE [13] assuming that RF pulses of constant fluence are normally incident on a semi-infinite plane with electrical and thermal characteristics of dry skin, with adiabatic (thermally insulated) boundary conditions. The pulses have the maximum fluence that is consistent with FCC limits, 18 kJ/m^2. All thermal properties in the model are taken from the IT'IS database [14] and used without modification.

The BHTE can be written:

$$k\nabla^2 T - \rho^2 C m_b T + \rho SAR = \rho C \frac{dT}{dt} \tag{1}$$

where T is the temperature rise of the tissue (°C) above the baseline (pre-exposure) temperature at the surface. The surface is exposed to a normally incident plane wave with power density I_o (W/m^2) with power transmission coefficient T_{tr} into the surface and energy penetration depth L.

The thermal parameters are

k = 0.37 W/(m °C) (thermal conductivity)
ρ = 1109 kg/m^3 (density)
C_p = 3390 J/(kg °C) (heat capacity)
m_b = 106 ml/(min kg) (blood perfusion parameter)

(Frequency-dependent parameters are in Table 2)

The BHTE has two intrinsic time scales characterizing convective cooling by blood flow (τ_1) and thermal conduction from the skin layer (τ_2):

$$\tau_1 = \frac{1}{m_b \rho}$$
$$\tau_2 = \frac{L^2 \rho C_p}{k} \tag{2}$$

The absorbed power density (Specific Absorption Rate or SAR) beneath the surface is

$$SAR = \frac{I_o(t) T_{tr}}{\rho L} e^{-z/L} \tag{3}$$

Eq. (1) was solved analytically for this one-dimensional model using a computer algebra program (Maple, Waterloo

TABLE 1. Overview of FCC, IEEE C95.1-2019 and ICNIRP (2020) limits above 1.5-2 GHz.

Standard/Guideline		MPE W/m^2	Averaging Time, min	Fluence Limit for Pulses kJ/m^2
FCC (1.5-100 GHz)	Occupational	50	6	18 (effective limit)
	Public	10	30	18 (effective limit)
IEEE C95.1-2019 Whole body exposure 2-300 GHz (ERL)	Restricted	50	30	(varies with pulse width)
	Unrestricted	10	30	(varies with pulse width)
				$tp^{1/2}$ (intense pulses 30-300 GHz)
Local exposure 6-300 GHz	Restricted	200 (6 GHz) to 100 (300 GHz)	6	
			6	$0.2\ tp^{1/2}$ (intense pulses 30-300 GHz)
	Unrestricted	40 (6 GHz) to 20 (300 GH)		
ICNIRP (2020) (2-300 GHz) Whole body exposure	Occupational	50 (2-300 GHz)	30	(varies with pulse width)
	General Public	10 (2-300 GHz)	30	(varies with pulse width)
Local exposure (6-300 GHz) (>6 min)	Occupational	200 (6 GHz) decreasing to 100 (300 GHz)	6	(varies with pulse width)
				(varies with pulse width)
	General Public	40 (6 GHz) decreasing to 20 (300 GHz)	6	

MPE: maximum permissible exposure; ERL: exposure reference level (refers to power density incident on skin). IEEE C95.1 defines local exposure as when "a limited portion of the body is subject to most of the incident energy" FCC does not have explicit limits on fluence but has limits on MPE and the averaging time imposes implicit limits on pulse fluence.

Maple, Waterloo ON), followed by numerical calculations using Matlab (Mathworks, Natick MA) and a finite element modeling program (FlexPDE, PDE Solutions, Spokane Valley, WA). Analytical solutions were also confirmed by a finite-difference-time-domain (FDTD) program at Nagoya Institute of Technology.

The solution to Eq. 1 to a suddenly imposed heat source Iou(t) (where u(t) is the Heaviside step function) is given by Eq. 4 (bottom of page) where erfc(x) is the complementary error function and T_{ss} is the steady state temperature increase at the surface

$$T_{ss} = \frac{I_0 T_{tr} L}{k(\tau_2/\tau_1 + \sqrt{\tau_2/\tau_1})} \tag{5}$$

The impulse response is the time derivative of the step response (Eq. 4)

$$T_{sur,impulse,normalized} = \frac{1}{\tau_1}\left(1+\sqrt{\frac{\tau_1}{\tau_2}}\right) e^{\left(\frac{1}{\tau_2}-\frac{1}{\tau_1}\right)t} erfc\left[\sqrt{\frac{t}{\tau_2}}\right] \tag{6}$$

The response to a very short pulse of fluence F is then F times $T_{sur,impulse,normalzed}$.

To avoid numerical overflow when evaluating Eqs. 4 and 6 for large t, the asymptotic expansion

$$e^x erfc\left(\sqrt{x}\right) \rightarrow \sqrt{\frac{1}{\pi x}} \quad \text{as } x \rightarrow \infty \tag{7}$$

was used, generally for times t > 200 sec. This approximation introduces errors below 5% for x > 10 and below 1% for x > 50.

In the present planar (1D) model, T_{tr} and L are calculated using dielectric data for dry skin [15] (Table 2).

Calculations were carried out for maximum fluence pulses consistent with FCC limits (18 kJ/m^2) of varying duration, for carrier frequencies between 1-300 GHz and exposure durations or pulse widths between 0.1-360 sec. In addition, the impulse response (Eq. 6) was scaled for the same fluence. The solutions were obtained analytically and verified separately by both finite element and FDTD simulations; the results were in very close agreement and would overlap indistinguishably in the figures below. The maximum fluence pulses, which are very intense pulses repeated no more than once per 6 or 30 minutes, provide upper limits to thermal transients

$$\frac{T_{sur}(t)}{T_{ss}} = 1 + \frac{\text{erfc}\left(\sqrt{\frac{t}{\tau_2}}\right) e^{-t/\tau_1 + t/\tau_2}(\tau_2 + \sqrt{\tau_1\tau_2})\text{-erfc}\left(\sqrt{\frac{t}{\tau_1}}\right)(\sqrt{\tau_1\tau_2}) + \tau_1)}{(\tau_1 - \tau_2)} \tag{4}$$

TABLE 2. Frequency-dependent parameters for dry skin.

Frequency (GHz)	L (m)Dry Skin	T_{tr}	τ_2 (sec)
1	1.92E-02	0.45	3760
3	9.43E-03	0.47	904
6	4.09E-03	0.48	170
10	1.90E-03	0.49	36
30	4.27E-04	0.54	1.85
94	1.87E-04	0.69	0.36
100	1.82E-04	0.70	0.34
300	1.40E-04	0.84	0.19

from more realistic RF pulses and are not themselves realistic exposures.

A. TRANSIENT TEMPERATURE INCREASES

Figs. 1-5 summarize the transient increases in surface temperature from these exposures together with the steady-state temperature increase from continuous exposure at 50 W/m^2 (the FCC limits for occupational exposure between 1.5-100 GHz) The steady-state temperature increases agree well with another study [16] using a much more detailed simulation of the body. At all frequencies, the transient temperature increases are bracketed by the impulse and steady state responses. The peak temperature increase at the end of each pulse can be approximated by the impulse response evaluated at the end of the pulse:

$$\Delta T \approx \frac{T_{tr} I_o t_p}{\rho C_p L} \operatorname{erfc}\left(t_p/\tau_2\right) e^{t_p/\tau_2}, \quad \tau_2 \ll \tau_1$$
$$\approx \frac{T_{tr} I_o}{\sqrt{\pi k \rho C_p}} t_p^{1/2}, \quad \tau_2 \ll t_p < \tau_1 \qquad (8a,b)$$

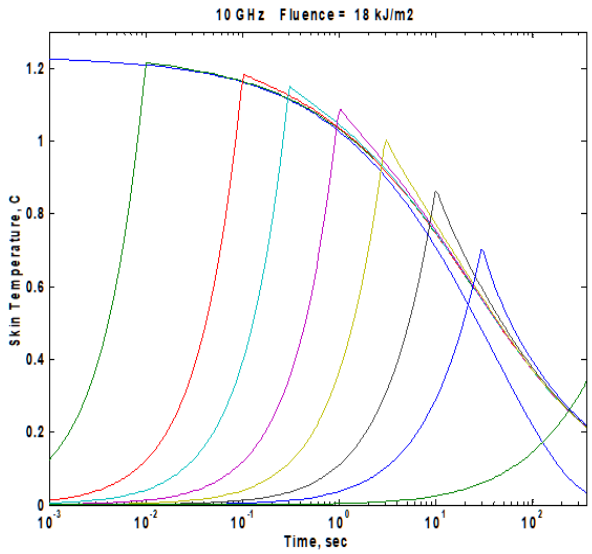

FIGURE 1. Incremental temperature increases ΔT for RF pulses of varying duration and constant fluence (18 kJ/m^2) at 10 GHz. From left: impulse, tp = 0.01, 0.1, 0.3, 1, 3, 10, 30 and 360 sec. (Io = 1800, 180, 60, 18, 6, 1.8, 0.6, 0.05 kW/m^2, respectively).

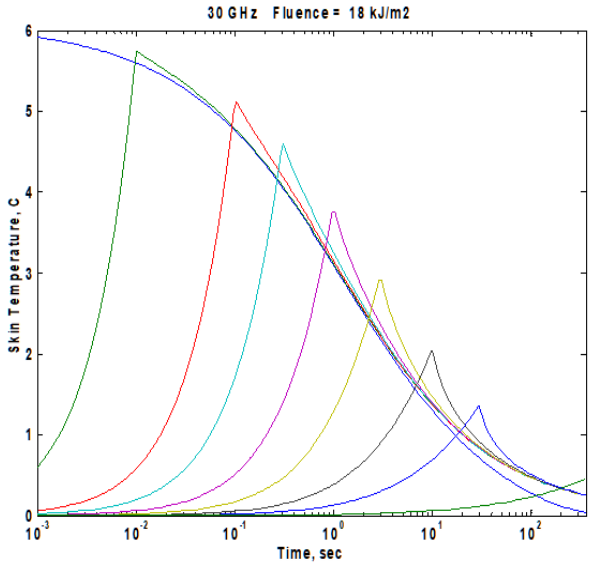

FIGURE 2. Incremental temperature increases ΔT RF pulses of varying duration and constant fluence (18 kJ/m^2) at 30 GHz. Pulse widths and incident power densities as in Fig. 1.

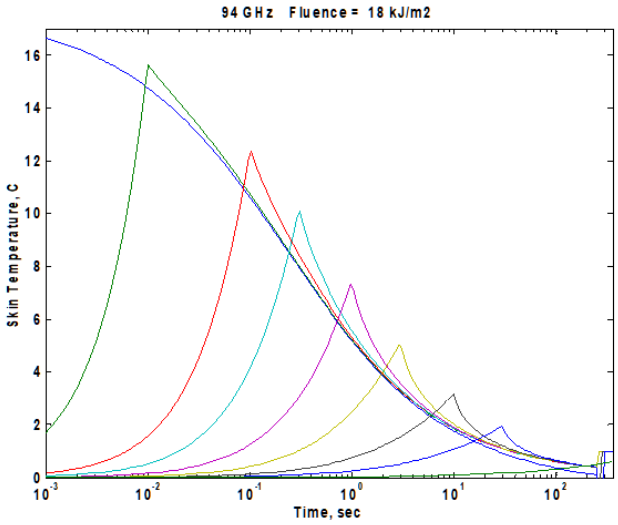

FIGURE 3. Incremental temperature increases ΔT for RF fluence pulses of varying duration and constant fluence (18 kJ/m^2) at 94 GHz. Pulse widths and incident power densities as in Fig. 1.

Particularly at the higher mm-wave frequencies, the peak temperature increases from these constant-fluence pulses can briefly become quite high. Implications of this for thermal hazards (thermal pain, burns) are discussed later in this paper.

B. MORE COMPLEX WAVEFORMS

The above discussion pertains to extreme but highly improbable exposures, i.e. a single very intense pulse repeated no more than once per averaging time. The implications of the model for more realistic waveforms can be examined by considering the BHTE as a lowpass filter relating the frequency spectrum of the amplitude modulation waveform (not the

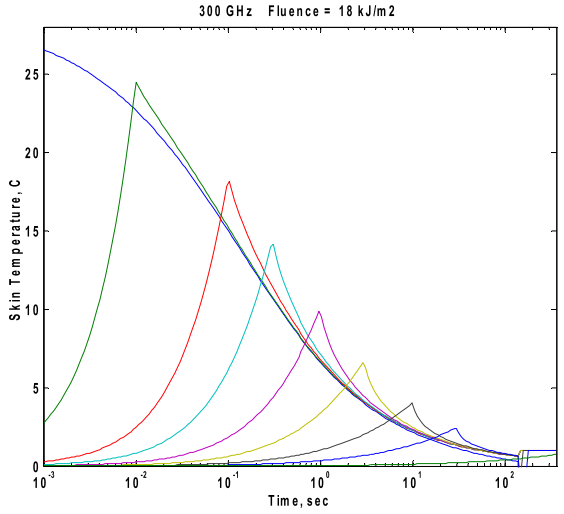

FIGURE 4. Incremental temperature increases ΔT for RF pulses of varying duration and fluence of 18 kJ/m^2 at 300 GHz. Pulse widths and incident power densities as in Fig. 1.

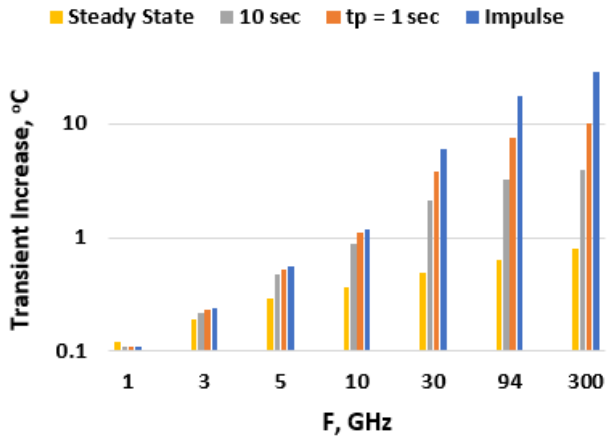

FIGURE 5. Transient temperature increases produced by 18 kJ/m^2 pulses of varying width at different frequencies. Also shown is the peak temperature increase for an impulse with same fluence, and the steady state temperature increase for an incident power density of 50 W/m^2.

frequency spectrum of the RF signal itself) to the temperature increase at the skin surface. The transfer function H(jω) is (Eq. 12 in [8])

$$\frac{T_{sur}(j2\pi f)}{I_0(j2\pi f)T_{ss}} \approx \frac{1}{\sqrt{1+s\tau_1}}, \quad \tau_1 \gg \tau_2 \tag{9}$$

where f refers to the frequency of the modulation waveform (not the carrier frequency) $s = j2\pi f$. Eq. 9 describes a half-order lowpass filter with a −3dB cutoff frequency of approximately $0.5/\tau_1$ (<1 mHz). This is far below the frequency spectra of amplitude modulation waveforms of communications or broadcasting signals. For example, the amplitude modulation waveforms of GSM cellular signals have frequency components at harmonics of 217 Hz [18] and such harmonics would produce very tiny fluctuations in skin temperature compared to the slow rise in skin temperature due to the time-averaged power density. Pulses from devices transmitting at high crest factors (e.g. Wi-Fi and radar) typically are brief and have low fluence (but perhaps high peak intensity) and likewise induce small thermal transients in skin at realistic exposure levels.

To illustrate, Fig. 6 shows the increase in skin temperature during a 6 min-exposure to square wave modulated radiation (94 GHz) with different periods but a constant time-averaged power density of 50 W/m^2, obtained by integrating the solution to Eq. 1 using the finite element method. The frequency spectrum of this waveform has components at odd multiples of the fundamental frequency of the waveform, 0.16 and 0.016 Hz, which are far above the cutoff frequency of the filter. The fluctuations in surface temperature are superimposed on a gradual increase due to the low-frequency (i.e. time averaged) component of the exposure. The dominant response time of the skin temperature is of the order of τ_1 (≈8 min) reflecting heat loss from subcutaneous tissue to the body core, not τ_2 (0.36 sec) that characterizes diffusion of heat from the skin layer. The short-term temperature fluctuations are suppressed by the very low cutoff frequency of the thermal response of skin.

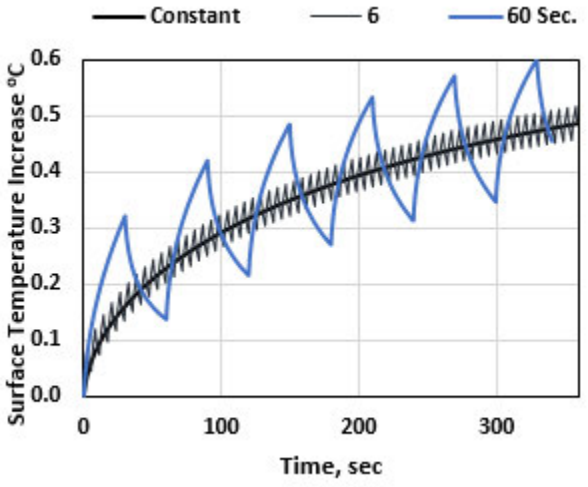

FIGURE 6. Variation in surface temperature from exposure to square wave modulated 94 GHz energy with periods of 6 and 60 sec at a constant time-average incident power density of 50 W/m^2. Also shown is the step response for Io = 50 W/m^2.

III. COMPARISON WITH EXPERIMENT

The thermal model can be validated with reference to experiments by Walters et al [18],together with data from a more recent but much smaller study by Parker *et al.* [19] Walters *et al.* exposed 10 subjects (7 males, 3 females) on their backs to 3-sec 94 GHz pulses with incident power densities ranging from 9-17.5 kW/m^2, while simultaneously measuring the increase in skin temperature using infrared thermography. Male subjects were shirtless, females wore

sports bras. The study was designed to determine the thresholds for thermal pain, using a staircase procedure involving multiple exposures close to the pain threshold. This resulted in >200 recordings of skin temperature vs. time in these subjects. The study did not record burns or other skin damage in the subjects.

Fig. 7 compares experimental and predicted results from [18], with each datapoint representing a single exposure to a single subject. The figures also shows recorded temperature increases from a later, and much smaller study, by Parker *et al.* [19]. In that study, 6 subjects were exposed to a single 3-sec pulse of 94 GHz mm-waves to their lower backs/buttocks to 3-sec pulses of RF energy at high levels, to produce minor skin damage (first degree burns). (Fig. 7 shows 4 data points. Data from one of the subjects had been discarded in the original study due to a technical problem and two data points overlap in the figure.)

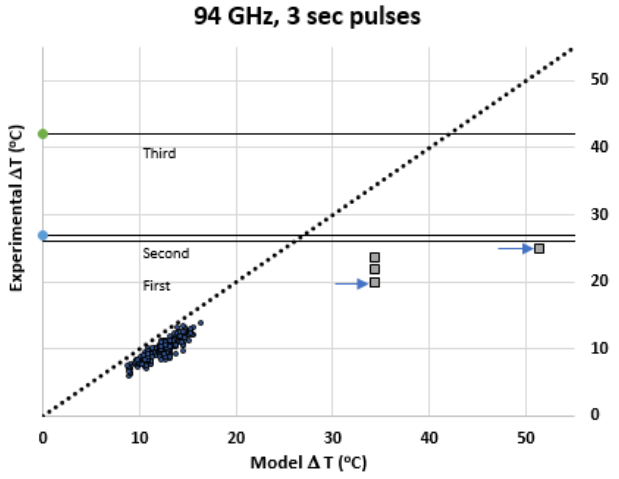

FIGURE 7. Experimental vs. calculated transient increases of skin temperature on backs of subjects exposed to 3-sec 94 GHz pulses of mm-waves, with fluence ranging from 27-52.5 J/m^2. (•) 226 separate exposures to the subjects [18], (■) single exposures to 5 subjects (two of the data points overlap) to 94 GHz pulses with reported fluence of 120-180 kJ/m^2 [19]. The arrows indicate the two exposures resulting in first degree burns to the subjects. The horizontal lines are the anticipated thresholds for first-, second-, and third-degree burns from the baseline skin damage (Arrhenius) model (Table 3).

From Fig. 7, it can be seen that the baseline 1D model agrees quite well with experimental data from [18] with no adjustment in its thermal parameters, notwithstanding a consistent overprediction by ≈20% relative to the experimental results. Differences relative to Parker's results [25] are much larger, a factor of 2-3.

A modest but consistent overprediction of the model with Walters' results [18] might have several explanations:

A. BOUNDARY CONDITIONS

The use of adiabatic boundary conditions with Eq. (1) will cause the model to overpredict skin temperature increases. The combined effects of convective heat transfer and evaporation of moisture from the skin can be modeled by imposing boundary conditions [21], [25], [26]:

$$-k\frac{\partial T_{surface}}{\partial z} = h(T_{skin} - T_{air}) + A_{evap}(T_{skin} - T_{air})^2 \quad (10)$$

where z is the coordinate axis normal to the skin, h is a convective heat exchange coefficient, and A_{evap} is an empirical parameter that models cooling by evaporation of skin moisture. (Eq. 10 disregards radiative losses to the environment, which are anticipated to be relatively smaller than convective and evaporative heat losses). Values for h from the literature vary widely, from 1-15 W/(m^2 °C), while Jean *et al.* [23] use 2 W/(m^2 °C^2) for A_{evap}. A finite element solution of Eq. 1 with these boundary conditions shows a 4% reduction in the peak skin temperature relative to the case of adiabatic boundary conditions from a 3-sec 94-GHz pulse with fluence of 45 kJ/m^2.

B. PARAMETER UNCERTAINTY

The parameter values used in this study were obtained from the IT'IS database and used without modification. The increase in skin temperature produced by a 3-sec pulse at 94 GHz can be approximated by (Appendix)

$$T_{Sur,cond}(t) \approx I_o T_{tr}\left(2\sqrt{\frac{t}{\pi\rho C_p k}} - \frac{L}{k}\right) (t > \tau_2) \quad (11)$$

The grouping of parameters ($\rho k C_p$) (which is conventionally termed the thermal inertia) is $1.4 \cdot 10^6$ watt^{2}s/(m^{4}K^2) using thermal parameters for skin from the IT'IS database. However, both the IT'IS database and Duck's extensive tabulation [24] give ranges of parameter values for these parameters that can support roughly a 50% variation of the thermal inertia. In addition, the thermal inertia of skin varies with location on the body and between subjects, and it increases by more than a factor of 4 with vasodilation [29]. Increasing the thermal inertia by 30% (for 3-sec pulses at 94 GHz) would reduce the skin temperature increase by 16%, while increasing L by 30% would reduce the skin temperature increase by 10%. While *post-hoc* adjustment of the model parameters could bring the model into close agreement with Walters' data, that would negate the usefulness of those experimental results to validate the model.

C. MODEL UNCERTAINTY

The model assumes a uniform half plane with thermal and electrical properties of dry skin. In fact, skin is heterogeneous, with different layers (stratum corneum, epidermis, dermis) as well as subcutaneous fat and muscle having different thermal and dielectric properties. Epidermis, in particular, is highly variable in water content and hence in thermal properties [26].

Physiological (blood perfusion) and anatomical (thickness of tissue layers) factors become increasingly significant with longer exposure times and largely determine the steady-state increase in skin temperature. More complex models, e.g. [6], [21] provide higher precision but also introduce more

parameters to adjust and lead to overfitting. Nevertheless, the baseline 1D model is remarkably successful for predicting skin temperatures from short term RF exposures without any adjustment of its parameters. This is chiefly because the early transient response is dominated by heat conduction over short distances in tissue.

IV. THERMAL HAZARDS

It is interesting to compare predictions of this simple baseline model with observed or calculated thresholds for thermal hazards (pain and burns). Few comparable data exist for thresholds for hazards of high-fluence mm-wave pulses. However, thermal injury from pulsed infrared (IR) energy has been extensively studied and sophisticated models have been developed that fit available data quite well. We compare these results to baseline models for mm-wave exposure without adjusting their parameters. To the extent possible, we compare mm-wave exposures with IR exposures with similar pulse duration and energy penetration depth in tissue, and select IR data from the experiments with the largest available spot size (to better approximate a 1D exposure).

A. CUTANEOUS PAIN SENSATIONS

Averaged over all of the subjects, Walters *et al.* reported [18] that the mean threshold pulse fluence for ''prickling pain'' was 37.5 ± 1.5 kJ/m^2 (for 3-sec pulses at 94 GHz). The corresponding mean increase in skin temperature was 9.9 °C above the mean pre-exposure skin temperature of 34.0 °C (mean skin temperature at threshold for pain was 43.9 °C).

Different experimental techniques yield variable results. Park *et al.* [27] applied a thermal stimulating probe to different body sites of 16 young male subjects and determined thresholds for cutaneous thermal pain sensation ranging from 45-49 °C. The thresholds varied with the region of the body (the upper part of the body is generally more sensitive than lower parts of the body). Since the baseline skin temperature in those subjects was between 32-35 °C, this corresponds to about a 10 °C increase in skin temperature at the threshold for cutaneous thermal pain, but the thresholds vary considerably. Liu *et al.* reported that the skin temperatures in clothed human subjects in room environments ranged from 31-39 °C [28], which suggests that an increase in skin temperature of 5-13 °C would approach a 44 °C threshold for pain, depending on environmental conditions. In addition, an individual's sensitivity to cutaneous thermal pain depends on factors such as ''attention, vigilance, anxiety, personality and sociocultural background'' [29] as well as variations in neural sensitivity. We conclude that a 10 °C increase in skin temperature is a nominal threshold for cutaneous pain sensations but depending on individual circumstances the threshold can vary by up to a factor of 2 in either direction.

Fig. 8 shows the calculated fluence of pulses sufficient to raise skin temperature by 10 °C. The figure also summarizes the lower threshold for producing thermal pain from exposure to pulsed far infrared energy (FIR) which is absorbed very close to the skin surface [30]. The calculated thresholds from the baseline are similar to measured thresholds for far infrared energy, both in their dependence on pulse width and in the numerical values themselves. Comparisons for lower frequencies (below 94-300 GHz) are limited due to lack of data.

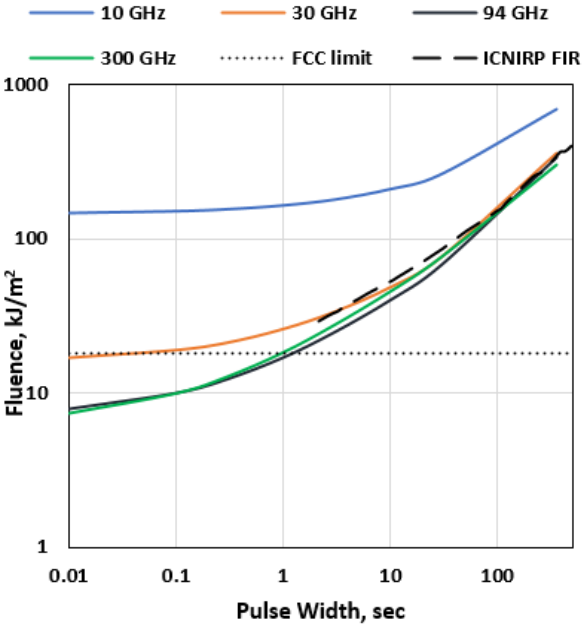

FIGURE 8. Pulse fluence that will produce a transient increase in skin temperature by 10 °C, considered as an approximate threshold for thermal pain. Also shown (coarse dashed line) is a summary of lower thresholds to produce thermal pain from long wavelength infrared energy, from a report by ICNIRP [30]. The fine dotted line is the maximum fluence of RF pulses consistent with FCC limits for both general-public and occupational exposures between 1.5-100 GHz.

B. BURNS

Thermal pain (which involves neural processes beginning with activation of nociceptors in the skin) which occurs quickly when excessive skin temperature develops. By contrast, thermal damage to tissue results largely from protein denaturation, which takes time to develop. Consequently there is an inverse relation between the time required for a burn to be produced, and the temperature of exposure.

The standard model for thermal damage to skin uses an Arrhenius function to quantify the rate of thermal damage:

$$\Omega = \int_{\tau=0}^{t} A e^{-\frac{\Delta E_a}{RT(\tau)}} d\tau \tag{12}$$

where T(t) is the temperature of the tissue (°K), R is the ideal gas constant, and A and ΔE_a are constants that are conventionally interpreted as a molecular collision frequency and the activation energy for protein denaturation. The integrand of Eq. 12 is the rate of thermal damage, which is integrated to yield Ω to quantify the extent of thermal damage.

As with the baseline thermal skin heating model discussed above, we use a standard set of parameters to create a baseline thermal damage model, and do not adjust the parameter

values to fit the very scant available data. For skin damage studies, the most commonly used parameters are $A = 3.1 \cdot 10^{98}$ sec^{-1} and $\Delta E_a = 6.27 \cdot 10^5$ J/mol, based on classical studies by Moritz and Henriques in the late 1940s [31]. The parameter values were chosen such that $\Omega = 0.53$, 1, and 10^4 represent nominal thresholds for first-, second-, and third-degree burns, respectively (Table 3). Eq. 12 is closely related to another measure of thermal dose, CEM43, but is more convenient to use with skin damage studies and historically has been the preferred model for such studies [32].

The damage parameter Ω quickly becomes very large when the skin temperature exceeds $\Delta E_a/R$. To simplify, we move $(A \cdot 1$ sec) into the exponent of Eq. 12 and express the skin temperature as an increase ΔT_{sur} above the baseline skin temperature of 307.16 °K (34 °C). The exponential takes on the value of 1 when

$$\Delta T_{sur} = \frac{\Delta E_a}{R \ln(A \cdot 1 \text{ sec})} - 307.16\,^{o}\text{K} \qquad (13)$$

This occurs at $\Delta T_{sur} = 25.4$ °C for the parameter values presently assumed. In other words, suddenly raising skin temperature from baseline by 25.4 °C and holding it at that temperature for 1 sec would result in $\Omega = 1$ (nominal threshold for second degree burn). Thresholds for first- and second-degree burns are quite close and considerably below those for third-degree burns.

For exposures to brief, high-fluence pulses, the integrand in Eq. 12 is sharply peaked at the point of highest skin temperature, at the end of the pulse (Fig. 9). Calculated threshold fluences and peak temperature increases (Eq. 12) for first-degree burns ($\Omega = 1$) for 3-sec 94-GHz pulses are summarized in Table 3.

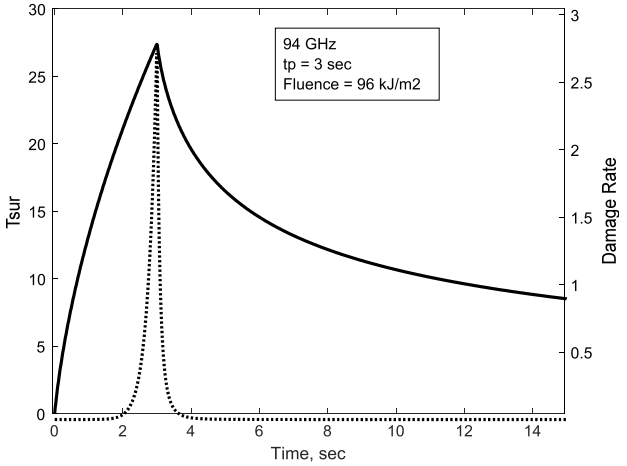

FIGURE 9. Temperature increase (solid line, axis left) and rate function (integrand of Eq. 12) (dotted line, axis right) for a 94-GHz pulse at threshold for producing a second-degree burn (fluence = 96 kJ/m^2).

These thresholds are nominal values only, calculated using the standard parameters used elsewhere for skin damage studies (pigs, humans). Alternate sets of parameters have been proposed for use in Eq. (12) to accommodate different

TABLE 3. Predicted thresholds for thermal damage to skin exposed to 3-second pulses of 94-GHz mm-waves.

Burn Degree	Damage to	Ω	Fluence kJ/m^2	ΔT_{sur}
1	Dermis	0.53	92	26
2	Epidermis and part of dermis	1	96	27
3	Full Thickness (Epidermis and Dermis)	10^4	148	42

damage endpoints or animal species (e.g. [33] and would produce varying threshold temperatures for thermal damage.

Jean *et al.* [23] showed the general usefulness of the Arrhenius thermal damage model by fitting 93 sets of threshold damage data for pulsed IR energy to the equivalent of Eq. (12). The data spanned a wide range of exposure parameters (IR wavelength, spot size, beam profile, pulse duration, energy penetration depth into tissue). Overall, the model fitted the data quite well, although in some cases the experimental data varied from calculated damage thresholds by factors up to 0.5 to 1.8. In part these variations may have been due to varying experimental methods or intersubject variability rather than to deficiencies in the model itself. Thermal damage thresholds are conventionally reported in terms of the ED_{50} (median effective dose resulting in a lesion of a specified nature in 50% of the exposed subjects), and are subject to considerable experimental variability.

Fig. 10 summarizes injury thresholds ($\Omega = 1$) for mm-wave pulses estimated using the baseline thermal damage model assuming a pre-exposure skin temperature of 34 °C. For comparison, Fig. 10 shows one set of damage thresholds from pulsed infrared energy of similar penetration depth in tissue as 94 GHz mm waves [34], which is in general agreement with expectations based on the baseline thermal damage model. A more precise model would take into account factors such as the beam pattern and spot size of the IR exposure together with anatomical details of skin, and is beyond the scope of the present study.

Apparently the only available data for thermal damage to skin from mm-wave pulses is in a 2016 technical report by Parker *et al.* [19]. The investigators exposed the lower backs/buttocks of 6 human subjects to 3-sec pulses of 94-GHz energy of two intensities (40 and 60 kW/m^2) corresponding to pulse fluences of 120 and 180 kJ/m^2. At the lower power density, thermal lesions (first degree burns) were produced in one of four exposed subjects, while the single subject exposed at the higher level developed a first-degree burn. (Data from a 6th subject was discarded due to technical problems)

These injuries were associated with peak temperature increases of 19.9 and 25 °C, corresponding to peak skin temperatures of 50.9 and 59.3 °C. The temperature increases at the lower exposure level are somewhat below anticipated

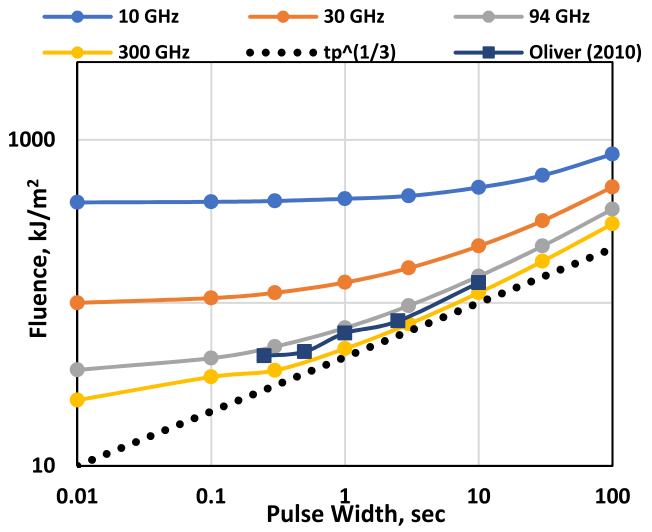

FIGURE 10. Pulse fluence resulting in $\Omega = 1$ (nominal threshold for second degree burn) vs. frequency and pulse width, calculated from present 1D model. Also shown (■) are data from Oliver (2010) [36[Error! Bookmark not defined.] for thresholds for minimal visual lesions in pig skin from pulsed infrared radiation (1940 and 2000 μm) with spot sizes 1.47-1.8 cm in diameter. Dotted line shows an exponential function (slope = .33) that approximates the thermal damage threshold vs. pulse width for mid- and far- infrared radiation of very short penetration depth [34].

thresholds for first degree burns based on the baseline thermal damage model (Table 3) while that at the higher exposure level was close to the anticipated threshold for first degree burn (Fig. 7). These temperature increases are generally in line with other reported thresholds for minor skin burns.

However, the reported temperature increases are considerably lower than would be expected based on other experimental data ([18]) and from the baseline thermal model (Fig. 7). The reported exposures in [19] should have raised skin temperature by more than 30 or 40 °C (Fig. 7), causing second or third degree burns.

The explanation for this difference is not clear. The experimental methods and exposure assessment in [19] are only briefly documented, and significant errors in dosimetry cannot be excluded.

If Parker *et al.* did produce a lesion from an exposure that raised skin temperature by 19.9 °C, that would imply thermal damage thresholds only a factor of two above pain thresholds reported in [18]. Based on the average temperature increase of 9.9 °C from an average exposure of 37.5 kJ/m^2, that study leads us to expect a threshold of about 75 kJ/m^2 for causing a first-degree burn (by scaling up the reported exposure in [18] by (19.9/9.9). The anticipated threshold for second degree burns would not be much higher. Since pulses used in [18] are representative of those used in the Active Denial system, that implies that the difference in exposure between one that causes pain and one that creates a burn might be rather modest compared to other uncertainties in exposure.

In a later paper [12], Parker *et al.* state that the threshold for producing a second degree burn from 3-sec 94 GHz pulses is 200-300 kJ/m^2. From the scant available data, it seems that the actual threshold is almost certainly much lower than that. Since thermal-damage thresholds are needed to assess the safety of mm-wave nonlethal weapons, a larger study would be needed, with sufficient statistical power to allow a meaningful analysis to define the ED_{50} for skin burns, which is the accepted quantity for reporting damage thresholds. Since thresholds for burn will undoubtedly vary with the individual, as well as with environmental conditions and type of clothing (both of which affect skin temperature), such factors would need to be considered as well. Perhaps such data exist but they do not seem to be readily available.

V. RELEVANCE OF MODEL TO EXPOSURE LIMITS

Table 4 summarizes the limits in the three exposure guidelines (FCC, IEEE, and ICNIRP) as they pertain to fluence of mm-wave pulses. ICNIRP limits for pulsed mid – and long-wavelength infrared exposure to skin [35] will be discussed for comparison as well.

Fig. 11 compares fluence limits in IEEE C95.1-2019, ICNIRP (2000) and FCC (1997) for mm-wave pulses with fluences for brief mm-wave pulses at 300 GHz that would cause a transient 10 °C rise in skin temperature. Additionally, ICNIRP (2013) limits are shown for mid- and far IR pulses from lasers.

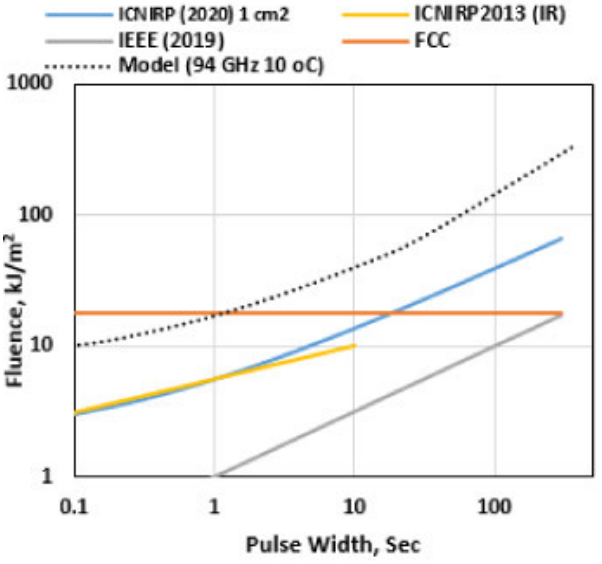

FIGURE 11. Limits on pulse fluence for local (partial body) exposures. ICNIRP (2020) applies to local exposures of less than 6 min and to skin areas of 1 cm^2 (limits are for occupational exposures at 300 GHz); IEEE C95.1-2019 applies to local exposures 30-300 GHz (restricted conditions, equivalent to occupational limits); ICNIRP (2013) applies to pulsed IR energy (wavelength 100 μm). Also shown is the maximum fluence for pulses allowed by FCC limits (general public or occupational) (1.5-100 GHz). The dotted line shows the calculated fluence (from the baseline thermal model) of pulses at 94 GHz that would produce a 10 °C transient rise in skin temperature, considered to be the threshold for thermal pain. Such pulses would comply with FCC limits if shorter than 1 sec.

FCC does not explicitly limit the fluence of intense RF pulses, but the combination of MPE (10 and 50 W/m^2 for general public and occupational limits) combined with the

TABLE 4. Exposure limits for pulse fluence.

		Incident energy density kJ/m^2	Averaging Area
ICNIRP (2020)** (30< f_G <300 GHz)	Occupational	$275/f_G^{0.177}$ x 0.36[0.05+0.95(t/360)$^{0.5}$] $275/f_G^{0.177}$ x 0.72[0.025+0.975(t/360)$^{0.5}$]	4 cm^2 (2 cm×2 cm) 1 cm^2 (1 cm×1 cm)
	General public	$55/f_G^{0.177}$ x 0.36[0.05+0.95(t/360)$^{0.5}$] $55/f_G^{0.177}$ x 0.72[0.025+0.975(t/360)$^{0.5}$]	4 cm^2 (2 cm×2 cm) 1 cm^2 (1 cm×1 cm)
IEEE C95.1-2019 (30< f_G <300 GHz)	Restricted Unrestricted	1 $t^{0.5}$ 0.2 $t^{0.5}$	1 cm^2 1 cm^2
FCC (1.5-100 GHz)	Occupational General Public	18 18	
ICNIRP (2013) (laser)*** (2600 nm < λ <1 mm)		5.6 $t^{0.25}$ (1 ns-10 s)	diameter of 11 mm, λ >1.4 μm
(1400 nm < λ <1 mm)		1 kW/m^2 (10s -30000s) 100 W/m^2	diameter of 3.5 mm, λ >100 μm Exposed area < 0.01 m^2 Exposure area > 001 m^2

averaging times (30 and 6 min, respectively) implicitly limits pulse fluence to 18 kJ/m^2 for both occupational and general public exposure. Fig. 11 suggests that short (<1 sec) pulses at 300 GHz might have sufficient fluence to raise skin temperature by 10 °C but would comply with the FCC MPE. Such pulses would remain well below thresholds for producing burns. Such extreme exposures are virtually never encountered in the real world (apart from targets of mm-wave nonlethal weapons) and, for practical purposes, the FCC limits are protective against the thermal hazards considered here.

FCC has recently proposed to modify its rules to address the possibility of excessive thermal transients from brief, high-fluence RF pulses by applying ''device-based'' time-averaging to portable devices. Device-based (or source-based) averaging has long been incorporated in FCC rules, applied for example to compliance testing of GSM cellular handsets whose duty cycle of transmission is inherently limited by GSM modulation [36]. For other devices, e.g. a Wi-Fi router, compliance has to be established assuming the maximum possible duty cycle, which approaches 100% even though the actual duty cycle of transmission is ordinarily very low. FCC has proposed to extend ''device-based time-averaging'' to a device that can ''actively track its RF emissions while limiting potential temperature rise in tissue due to an impulse to value of about 0.1 °C'' [37]. This is clearly an extremely conservative benchmark in relation to health and safety hazards of RF energy.

The document explains:

''…since we do not limit temporal-peak SAR or power density, all the energy available in a time-averaging period could be deposited in a moment resulting in a well-defined temperature rise and be compliant with the rules. Thus, using the extended time-averaging periods of 6 minutes or 30 minutes set forth in our rules in other contexts or either of the alternative time windows specified by ICNIRP and IEEE could allow for inappropriate temperature rises in extreme cases when intense exposure occurs only for a brief period.''

This rule in effect limits the fluence of pulses incident on the body to the ''device based averaging time'' times the MPE (10 or 50 W/m^2). Figure 12 summarizes the proposed FCC device-based averaging times in different frequency ranges and resulting incremental temperature increases either under worst-case exposures (impulses at maximum allowable fluence) or constant exposure at the MPE. These increases will bracket those produced by pulses of intermediate duration. (Fig. 12 is based on the occupational MPE; the corresponding temperature increases based on the MPE for the general public will be a factor of 5 smaller.)

The device-based averaging time, in combination with the MPE, does in fact, limit transient temperature increases to 0.1 °C for worst-case (impulse) exposures based on occupational exposure limits (Fig. 12). However, these transients are superimposed on larger and slower increases in surface temperature due to the average exposure, a result of the extreme lowpass thermal response of skin. For this slower and larger response, the response time is of the order of τ_1 (several minutes) and the existing 6-minute averaging time is appropriate.

To illustrate, Fig. 13 shows the increase in surface temperature produced by a sequence of maximum-fluence (50 J/m^2) impulses at 100 GHz repeated once per ''device-based averaging time'' of 1 sec. Each pulse produces a transient increase in skin temperature of ≈0.05 °C, compared to the steady-state increase in temperature of 0.65 °C. Increases based on general-public MPE will be a factor of 5 smaller.

This ''device-based time averaging'' is extremely conservative, since it is based on a mathematical worst-case exposure (maximum-fluence impulses) and it is designed to limit incremental temperature increases to levels far below

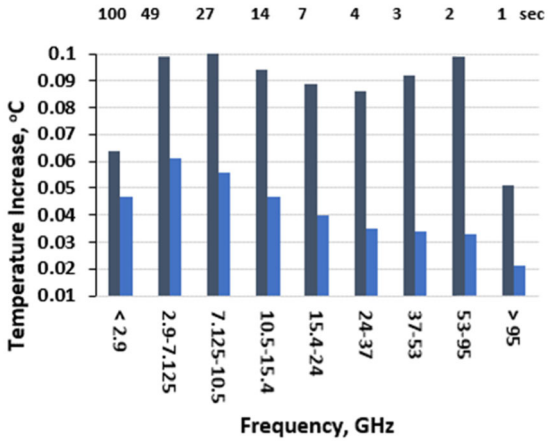

FIGURE 12. Transient temperature increases produced by pulses with fluence equal to the FCC MPE (occupational limits) times the "device-based-averaging time". Top row: "device based" averaging time in each frequency range. Black columns: incremental temperature increase produced by maximum fluence impulses (calculated at the frequency at the upper end of the indicated frequency band). Blue columns: incremental temperature increase from constant exposure at the MPE (occupational limits) for the duration of the device-based averaging time. For calculations for the highest frequency bin, a frequency of 100 GHz was assumed. Results were calculated on the basis of occupational limits; corresponding increases for limits for the general public would be a factor of 5 smaller.

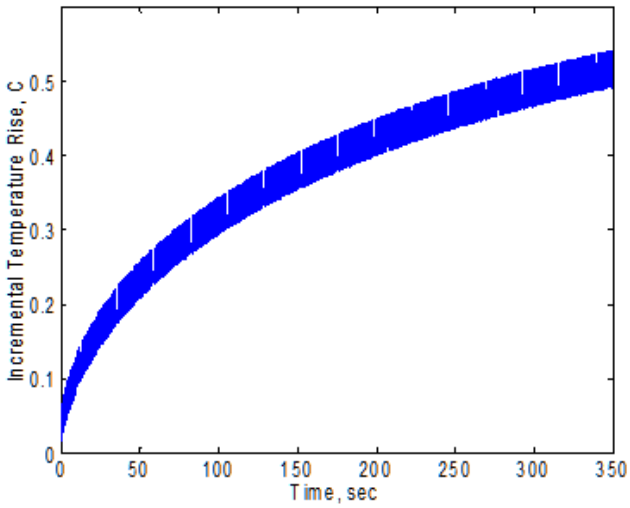

FIGURE 13. Thermal response to train of maximum-fluence pulses (50 J/m^2) at 100 GHz, repeated once per device-based averaging time (1 sec). Each pulse produces a transient increase in skin temperature of about 0.05 °C, while the train of pulses produces a slowly growing increase in temperature that approaches a steady state temperature of 0.65 °C, the same as for a continuous exposure at the MPE (50 W/m^2).

identified hazards. This approach is inefficient, in that it would exclude devices that produce exposures that exceed the MPE during occasional device-based averaging times but comply when exposure is averaged over the time periods (6 or 30 min) specified in the MPE. That would exclude, for example, a device that transmits 100 GHz and produces exposures to the body that comply with the MPE averaged over 6 min but exceeds the MPE in one or more 1 sec intervals. If the goal is to protect against excessive thermal transients from extreme high-fluence mm-wave pulses, however unrealistic such exposures may be, a more efficient approach would be to limit pulse fluence directly, as an add-on to existing limits and averaging times. This is the approach taken in the latest revisions of IEEE C95.1-2019 and ICNIRP (2020).

VI. DISCUSSION

The simple 1D model is remarkably successful in accounting for transient temperature increases from pulsed mm-wave energy without adjustment of any parameters. It shows that thermal transients from pulsed mm-waves that comply with FCC exposure limits are too small to be significant for health and safety with the possible exception of extreme high-fluence pulses that are mathematically compliant with the limits, that can produce peak increases in skin temperature that might elicit cutaneous thermal pain but not cause burns.

A separate issue, not explored here, is heating from highly focused exposures on the skin, for which a simple 1D model would not be appropriate. Other effects, such as the possible increase in mm-wave absorption by the body due to clothing [38], or nonuniform exposures, for example to the eye, from diffraction effects at mm-wave frequencies warrant further investigation and may lead to further refinement of the exposure limits.

There has been a striking difference in approach in setting exposure limits for far infrared (FIR) radiation (0.05-1 mm wavelength) vs. RF radiation, in part due to different technological characteristics of major sources of exposure. The far infrared lies just above the mm-wave band in frequency, energy in both parts of the spectrum is absorbed close to the skin surface, and the biophysics of skin heating in both cases is similar. However, pulsed infrared sources (lasers) are widely used, and often operate at very high peak power levels. The ICNIRP FIR guidelines for skin are based on injury thresholds for short pulses (up to 10 sec), to avoid injury from brief exposures such as from a laser beam. These limits are based on extensive experimental data for pulsed-IR injury thresholds. Such data are presently lacking for mm-waves, in part due to the absence of high-powered pulsed mm-wave sources apart from specialized (and to date, largely or entirely unused apart from testing) nonlethal weapons. By contrast, ICNIRP FIR limits for longer exposures >10 sec. are based on "thermal stress" considerations and are 100 or 1000 W/m^2 depending on the exposed area of skin. These were motivated in part by use of radiant warmers, infrared warming cabins and "infrared saunas" used by ordinary consumers. Exposure limits for FIR radiation from such devices are far less conservative than RF exposure limits since the devices were designed to heat skin. It is safe to say that people are frequently exposed to infrared energy, from heat lamps, cooking appliances, infrared saunas, infrared space heaters, as well as from simply sitting near a fireplace, that far exceed

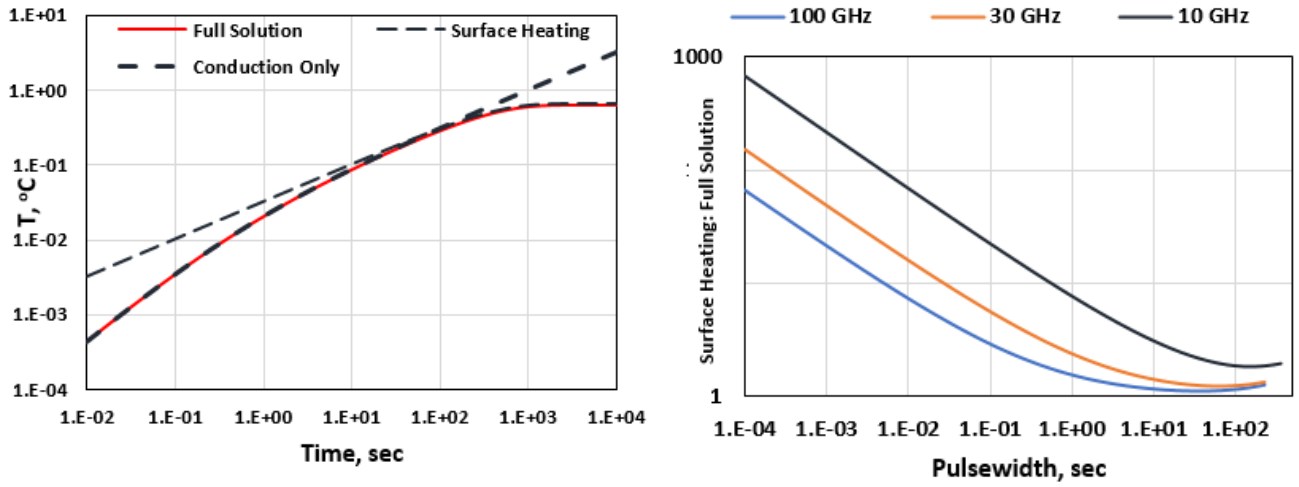

FIGURE 14. (a). Conduction only, surface heating, and full solutions for step response compared, 94 GHz, Io = 50 W/m^2. The full solution and conduction-only solutions overlap for short times, while the full solution and surface heating approximation overlap for long times. (b). Ratio of surface heating approximation to full solution for incremental temperature increases produced by pulses of indicated duration. Same values for thermal parameters as used elsewhere in this study. The decrease in surface temperature for the full solution at long times is due to effects of blood perfusion. The surface heating solution significantly overestimates the incremental increase in surface, temperature from brief pulses, more so at lower frequencies.

FCC limits for mm-waves, even though the defined hazards for both parts of the spectrum are the same.

APPENDIX
COMMENTS ON APPROXIMATIONS TO BIOHEAT EQUATION

Many authors have used the bioheat equation (Eq. 1) to model the thermal response of tissue to radiant heating, including in the context of setting exposure limits. While numerical image-based models of the body provide much greater detail, simplified "baseline" models are useful to study parametric relations and help interpret numerical results. Given that analytical solutions of the BHTE, even for simple cases, are mathematically cumbersome, various simplified approximations to the full analytical solutions are useful. We comment on the validity and range of usefulness of two such approximations as they apply to the step response (Eq. 2) of the 1D model.

Conduction only approximation ($m_b \rightarrow 0$) for which the BHTE reduces to the simple heat conduction equation. The step response of the 1D model can be written

$$T_{Sur,cond}(t) = \frac{I_o T_{tr} L}{k}\left[2\sqrt{\frac{t}{\pi\tau_2}} + \left(e^{\frac{t}{\tau_2}}\, erfc\left(\sqrt{t/\tau_2}\right) - 1\right)\right]$$
$$\approx I_o T_{tr}\left(2\sqrt{\frac{t}{\pi\rho C_p k}} + \frac{L}{k}\left(\sqrt{\frac{\tau_2}{\pi t}} - 1\right)\right) (t > \tau_2)$$
$$\rightarrow \frac{I_o T_{tr} t}{kL\rho C_p} \quad \text{as } t/\tau_2 \rightarrow 0 \qquad \text{(A1)}$$

Eq. A1 has no finite steady state solution in the 1D model. In the early transient period ($t \ll \tau_1$) the step response (Eq. A1) is virtually identical to the full solution (Eq. 4, main paper).

Surface heating approximation ($L \rightarrow 0$) is obtained by deleting the source term in Eq. 1 and forcing a thermal gradient $-I_o T_{tr}/ks$ at the surface (where s is the Laplace variable). The step response of this model is

$$T_{sur} = \frac{I_o T_{tr} L}{k}\sqrt{\frac{\tau_1}{\tau_2}}\, erf\left(\sqrt{\frac{t}{\tau_1}}\right) \qquad \text{(A2)}$$

with asymptotic expansion for small t

$$T_{sur} = \frac{2 I_o T_{tr}}{\sqrt{\pi k \rho C_p}}\sqrt{t} \quad \text{as } t \rightarrow 0 \qquad \text{(A3)}$$

This coincides with the first term in Eq. 8. For constant-fluence pulses of fluence F this becomes

$$T_{sur} \rightarrow \frac{2 F T_{tr}}{\sqrt{\pi k \rho C_p t}} \qquad \text{(A4)}$$

This diverges for very short pulses (i.e. as $t_p \rightarrow 0$), a consequence of pushing a finite amount of energy into an infinitesimal volume of tissue. For long times ($t > \tau_1$), Eq. A2 becomes

$$T_{sur} \rightarrow \frac{I_0 T_{tr} L}{k(\sqrt{\tau_2/\tau_1})} \quad \text{as } t \rightarrow \infty \qquad \text{(A5)}$$

The ratio R of the surface heating approximation to the full analytical solution in the steady state is

$$R = \frac{\tau_1 - \tau_2}{\tau_1 - \sqrt{\tau_1 \tau_2}}$$
$$\approx 1 + \sqrt{\tau_2/\tau_1} \quad \text{if } \tau_2 \ll \tau_1 \qquad \text{(A6)}$$

and consequently, the surface heating approximation approaches the full analytical solution at long times.

Figure 14 compares the step responses of the two approximations with the full analytical solution of the BHTE. The

surface heating approximation fails badly for early transient responses but is quite good at long times, while the conduction-only solution fails badly for long times because it ignores the effects of blood perfusion. Both approximations are more compact mathematically and easier to probe for their dependence on parameters of the problem than the full analytical solution to the BHTE.

The authors thank Drs. Achim Enders, Karl Schulmeister, and Bruce Stuck for discussions during the course of this work.

REFERENCES

[1] International Commission on Non-Ionizing Radiation Protection, "Guidelines for limiting exposure to electromagnetic fields (100 kHz to 300 GHz)," *Health Phys.*, vol. 118, no. 5, pp. 483–524, 2020.

[2] *IEEE Standard for Safety Levels With Respect to Human Exposure to Electric, Magnetic and Electromagnetic Fields, 0 Hz to 300 GHz*, Standard 1-2019, 2019.

[3] *Evaluating Compliance with FCC Guidelines for Human Exposure to Radiofrequency Electromagnetic Fields*, Federal Communications Commission, Washington, DC, USA, 1997.

[4] *Radiofrequency Electromagnetic Fields-Properties, Quantities and Units, Biophysical Interaction, and Measurements*, National Council on Radiation Protection and Measurements, Bethesda, MD, USA, 1981.

[5] E. Neufeld and N. Kuster, "Systematic derivation of safety limits for time-varying 5G radiofrequency exposure based on analytical models and thermal dose," *Health Phys.*, vol. 115, no. 6, pp. 705–711, Dec. 2018.

[6] E. Neufeld, T. Samaras, and N. Kuster, "Discussion on spatial and time averaging restrictions within the electromagnetic exposure safety framework in the frequency range above 6 GHz for pulsed and localized exposures," *Bioelectromagnetics*, vol. 41, no. 2, pp. 164–168, Feb. 2020.

[7] K. R. Foster, M. C. Ziskin, and Q. Balzano, "Thermal response of human skin to microwave energy: A critical review," *Health Phys.*, vol. 111, no. 6, pp. 528–541, Dec. 2016.

[8] K. R. Foster, M. C. Ziskin, Q. Balzano, and A. Hirata, "Thermal analysis of averaging times in radio-frequency exposure limits above 1 GHz," *IEEE Access*, vol. 6, pp. 74536–74546, 2018.

[9] M. C. Ziskin, S. I. Alekseev, K. R. Foster, and Q. Balzano, "Tissue models for RF exposure evaluation at frequencies above 6 GHz," *Bioelectromagnetics*, vol. 39, no. 3, pp. 173–189, Apr. 2018.

[10] J. E. Parker, E. J. Nelson, C. W. Beason, and M. C. Cook. (2017). *Effects of Variable Spot Size on Human Exposure to 95-GHz Millimeter Wave Energy*. [Online]. Available: https://apps.dtic.mil/dtic/tr/fulltext/u2/1037828.pdf

[11] S. Cazares, J. A. Snyder, J. Belanich, J. Biddle, A. Buytendyk, S. H. Teng, and K. O'Connor, "Active denial technology computational human effects End-To-End hypermodel (ADT CHEETEH)," *Hum. Factors Mech. Eng. for Defense Saf.*, vol. 3, no. 1, p. 13, Dec. 2019.

[12] J. E. Parker, E. J. Nelson, C. W. Beason, and M. C. Cook. (2017). *Thermal and Behavioral Effects of Exposure to 30 kW, 95-GHz Millimeter Wave Energy*. Accessed: Jun. 30, 2020. [Online]. Available: https://apps.dtic.mil/dtic/tr/fulltext/u2/1037054.pdf

[13] H. H. Pennes, "Analysis of tissue and arterial blood temperatures in the resting human forearm," *J. Appl. Physiol.*, vol. 1, no. 2, pp. 93–122, Aug. 1948.

[14] P. A. Hasgall, F. D. Gennaro, and C. Baumgartner. *IT'IS Database for Thermal and Electromagnetic Parameters of Biological Tissues. Version 4.0*. Accessed: May 15, 2018. [Online]. Available: www.itis.ethz.ch/database

[15] S. Gabriel, R. W. Lau, and C. Gabriel, "The dielectric properties of biological tissues: III. Parametric models for the dielectric spectrum of tissues," *Phys. Med. Biol.*, vol. 41, no. 11, p. 2271, 1996.

[16] K. Sasaki, M. Mizuno, K. Wake, and S. Watanabe, "Monte Carlo simulations of skin exposure to electromagnetic field from 10 GHz to 1 THz," *Phys. Med. Biol.*, vol. 62, no. 17, p. 6993, 2017.

[17] J. B. Andersen, P. E. Mogensen, and G. F. Pedersen, "Power variations of wireless communication systems," *Bioelectromagn. J. Bioelectromagn. Soc. Soc. Phys. Regul. Biol. Med. Eur. Bioelectromagn. Assoc.*, vol. 31, no. 4, pp. 302–310, 2010.

[18] T. J. Walters, D. W. Blick, L. R. Johnson, E. R. Adair, and K. R. Foster, "Heating and pain sensation produced in human skin by millimeter waves: Comparison to a simple thermal model," *Health Phys.*, vol. 78, no. 3, pp. 259–267, Mar. 2000.

[19] J. E. Parker, J. S. Eggers, and P. E. Tobin, "Thermal injury in human subjects due to 94-GHz radio frequency radiation exposures," General Dyn. Inf. Technol, San Antonio TX, USA, Tech. Rep. AFRL-RH-FS-TR-2016-0001, 2016. [Online]. Available: https://apps.dtic.mil/dtic/tr/fulltext/u2/a631765.pdf

[20] B. Chen, S. L. Thomsen, R. J. Thomas, and A. J. Welch, "Modeling thermal damage in skin from 2000-nm laser irradiation," *J. Biomed. Opt.*, vol. 11, no. 6, p. 64028, 2006.

[21] A. Kanezaki, A. Hirata, S. Watanabe, and H. Shirai, "Parameter variation effects on temperature elevation in a steady-state, one-dimensional thermal model for millimeter wave exposure of one-and three-layer human tissue," *Phys. Med. Biol.*, vol. 55, no. 16, p. 4647, 2010.

[22] D. Fiala, K. J. Lomas, and M. Stohrer, "A computer model of human thermoregulation for a wide range of environmental conditions: The passive system," *J. Appl. Physiol.*, vol. 87, no. 5, pp. 1957–1972, Nov. 1999.

[23] M. Jean, K. Schulmeister, and B. E. Stuck, "Computer modeling of laser induced injury of the skin," *Int. Laser Saf. Conf.*, vol. 2013, vol. 2013, no. 1, pp. 366–370.

[24] F. A. Duck, *Physical Properties of Tissues: A Comprehensive Reference Book*. New York, NY, USA: Academic, 2013.

[25] M. Lipkin and J. D. Hardy, "Measurement of some thermal properties of human tissues," *J. Appl. Physiol.*, vol. 7, no. 2, pp. 212–217, Sep. 1954.

[26] M. Gaáperin and ĐD. Juričič, "The uncertainty in burn prediction as a result of variable skin parameters: An experimental evaluation of burn-protective outfits," *Burns*, vol. 35, no. 7, pp. 970–982, Nov. 2009.

[27] S. Park, S.-H. Roh, and J.-Y. Lee, "Body regional heat pain thresholds using the method of limit and level: A comparative study," *Eur. J. Appl. Physiol.*, vol. 119, no. 3, pp. 771–780, Mar. 2019.

[28] Y. Liu, L. Wang, J. Liu, and Y. Di, "A study of human skin and surface temperatures in stable and unstable thermal environments," *J. Thermal Biol.*, vol. 38, no. 7, pp. 440–448, Oct. 2013.

[29] L. Plaghki and A. Mouraux, "How do we selectively activate skin nociceptors with a high power infrared laser? Physiology and biophysics of laser stimulation," *Neurophysiologie Clinique Clin. Neurophysiol.*, vol. 33, no. 6, pp. 269–277, Dec. 2003.

[30] I. C. O. N.-I. R. Protection, "ICNIRP statement on far infrared radiation exposure," *Health Phys.*, vol. 91, pp. 630–645, 2006.

[31] F. C. Henriques, Jr., and A. R. Moritz, "Studies of thermal injury: I. The conduction of heat to and through skin and the temperatures attained therein. A theoretical and an experimental investigation," *Am. J. Pathol.*, vol. 23, no. 4, p. 530, 1947.

[32] J. A. Pearce, "Relationship between Arrhenius models of thermal damage and the CEM 43 thermal dose," *Energy-Based Treatment Tissue Assessment*, vol. 7181, Feb. 2009, Art. no. 718104.

[33] B. Chen, S. L. Thomsen, R. J. Thomas, J. Oliver, and A. J. Welch, "Histological and modeling study of skin thermal injury to 2.0 μm laser irradiation," *Lasers Surgery Med.*, vol. 40, no. 5, pp. 358–370, Jul. 2008.

[34] J. W. Oliver, "Infrared skin damage thresholds from 1940-nm continuous-wave laser exposures," *J. Biomed. Opt.*, vol. 15, no. 6, p. 65008, 2010.

[35] I. Commission on Non-Ionizing Radiation Protection, "ICNIRP guidelines on limits of exposure to laser radiation of wavelengths between 180 nm and 1,000 μm," *Health Phys.*, vol. 105, no. 3, pp. 271–295, Sep. 2013.

[36] *Radio Frequency Radiation Exposure Evaluation: Portable Devices*, document CFR 2.1093(5), Sep. 1997.

[37] *Resolution of Notice of Inquiry, Second Report And Order, Notice of Proposed Rulemaking, And Memorandum Opinion And Order*, FCC, Washington, DC, USA, Nov. 2019.

[38] O. P. Gandhi and A. Riazi, "Absorption of millimeter waves by human beings and its biological implications," *IEEE Trans. Microw. Theory Techn.*, vol. 34, no. 2, pp. 228–235, Feb. 1986.